# Improved Macular Capillary Flow on Optical Coherence Tomography Angiography After Panretinal Photocoagulation for Proliferative Diabetic Retinopathy

AMANI A. FAWZI, ALAA E. FAYED, ROBERT A. LINSENMEIER, JING GAO, AND FEI YU

• PURPOSE: This study evaluated the macular microvascular changes in eyes with proliferative diabetic retinopathy (PDR) following panretinal photocoagulation (PRP).

• DESIGN: Using optical coherence tomographic angiography (OCTA), we prospectively studied 10 eyes of 10 subjects with high-risk PDR immediately before, at 1 month, and at 3-6 months following PRP, using a 3- × 3-mm OCTA scan at each visit.

• METHODS: The following parameters were calculated for the superficial (SCP), middle (MCP), and deep capillary plexuses (DCP): parafoveal vessel density (VD), adjusted flow index (AFI), and percent area of nonperfusion (PAN). Parafoveal SCP vessel-length density (VLD) was also evaluated. We performed univariate and multivariable statistics, adjusting for age and signal strength. To model the hemodynamic effect of PRP, we also present a mathematical model based on electrical circuits.

• RESULTS: We found no significant difference for the vascular density parameters following PRP, except for decreased density at the MCP at the latest timepoint in the adjusted multivariable model. PAN, a metric of nonperfusion adjusted for noise, and AFI, a surrogate metric of blood flow, showed significant increases at all capillary levels in the adjusted model. Our mathematical model explained how PRP would increase macular blood flow.

• CONCLUSIONS: Using OCTA, we found an overall increase in the flow metrics of all capillary layers in the macula following PRP, unrelated to macular edema or thickening, in line with the mathematical model. Our results suggest an overall redistribution of blood flow to the posterior pole following PRP, adding a new dimension to our understanding of the complex biologic effects of PRP in PDR. NOTE: Publication of this article is sponsored by the American Ophthalmological Society. (Am J Ophthalmol 2019;206:217–227. © 2019 Elsevier Inc. All rights reserved.)

Accepted for publication Apr 26, 2019.

From the Department of Ophthalmology, Feinberg School of Medicine, Northwestern University, Chicago, Illinois (A.A.F., A.E.F., R.A.L., J.G.); Department of Ophthalmology, Kasr Al-Ainy School of Medicine, Cairo University, Egypt (A.E.F.); Departments of Biomedical Engineering and Neurobiology, Northwestern University, Evanston, Illinois (R.A.L.); and Department of Biostatistics, University of California-Los Angeles, Los Angeles, California (F.Y.).

Inquiries to Amani A. Fawzi, Department of Ophthalmology, Feinberg School of Medicine, Northwestern University, 645 N. Michigan Avenue, Suite 440, Chicago, IL 60611; e-mail: afawzimd@gmail.com

THE GOAL OF LASER PANRETINAL PHOTOCOAGULATION (PRP) is to modify the natural history of proliferative diabetic retinopathy (PDR) by effecting regression of neovascularization. The basic pathophysiology of the therapeutic effect in humans is grounded in theory but confirmed by practice. Animal studies in laser-treated animal retinas have shown that PRP increases the flux of oxygen into the inner retina.[1–3] This is believed to be a result of decreased consumption by the laser-disrupted outer retina, especially photoreceptor inner segments, which are the highest consumers of oxygen in the body.[4] However, it is notable that animal models experimentally used to study lasers did not have a macula, and that these studies were done in nondiabetic models. In humans, the effect of PRP on retinal blood flow has been explored using various technologies in individual retinal blood vessels or the large retrobulbar and ocular vasculature.[5–10] These studies collectively showed large vessel constriction, increased flow speeds along with overall decreased blood flow following successful PRP treatment,[5–7] which did not occur when PRP was unsuccessful (eg, in subjects with poorly controlled diabetes).[9]

PDR is associated with the development of neovascularization and nonperfusion. The nonperfusion theoretically leads to increased peripheral vascular resistance, whereas neovascularization provides high-flow, low-resistance channels that counterbalance the increased peripheral resistance. These high-flow channels do not contribute to normal flow perfusion, as shown repeatedly in studies. PDR eyes have been shown to have an overall lower blood flow than normal or non-PDR eyes, which is consistent with the higher level of retinal ischemia and disease severity.[9,11–13] With regression of these neovascular and shunt vessels following PRP, normalization of flow in the macula is likely to reverse ischemia and decrease the stimulus for new blood vessel formation. Closure of intraretinal microvascular abnormalities and neovascularization would theoretically increase overall

0002-9394/$36.00
https://doi.org/10.1016/j.ajo.2019.04.032

resistance to flow, and, combined with the constriction of the large vessel in response to increased oxygen in the inner retina, collectively decrease the overall blood flow.

Although previous studies explored the large vessel effects of PRP, none addressed the microvascular retinal changes in a detailed fashion. The introduction of optical coherence tomography angiography (OCTA) has provided clinicians with a noninvasive tool to study 3-dimensional vascular capillary details. With progression of diabetic retinopathy, changes at the different capillary levels appear to be distinct, especially when considering the capillary blood flow.[14–16] Specifically, our studies showed that the blood flow at the deeper capillary plexuses (middle and deep, MCP and DCP) decline progressively with increasing retinopathy. Paradoxically, we found that the flow at the superficial plexus (SCP) showed no change or a trend of increasing with progression of retinopathy, consistent with dilated telangiectatic vessels and intraretinal microvascular abnormalities. We believed these SCP changes could be responsible for a "steal phenomenon," further exacerbating the ischemia at the deeper plexuses.[14,15]

With this in mind, we sought to explore the effect of laser PRP in subjects with high-risk PDR. We hypothesized that PRP would cause constriction of the large vessels, manifesting as a decrease in the overall SCP vessel density (VD), which includes the larger vessels. We also hypothesized that PRP would reverse the macular SCP steal phenomenon and modulate the macular capillaries, as well as induce relative normalization of blood flow with a decrease at the SCP and a commensurate increase at the deeper plexuses (MCP and DCP). To test this hypothesis, we performed a prospective study to compare the baseline OCTA measurement with serial follow-up measurements made at 1 and 3-6 months follow-up. We also present a mathematical model based on an electrical circuit model to simulate the retinal vascular and microvascular networks and the effect of PRP on microvascular flow in the macula.

## PATIENTS AND METHODS

THIS WAS A PROSPECTIVE ANALYSIS OF A CONSECUTIVE SERIES of all patients newly diagnosed with high-risk PDR[17] who received treatment with PRP in the course of their standard clinical care. The patients were recruited in the Department of Ophthalmology at Northwestern University in Chicago, Illinois between October 2017 and April 2018. The study was approved by the Institutional Review Board of Northwestern University. The study followed the tenets of the Declaration of Helsinki and was performed in accordance with Health Insurance Portability and Accountability Act regulations. Written informed consent was obtained from all participants.

• **PATIENT SELECTION:** Treatment-naïve eyes with high-risk PDR with no history of intravitreal pharmacotherapy, retinal laser treatment, or pars plana vitrectomy were eligible for this study. All patients underwent wide-field fundus fluorescein angiography at recruitment, using a California imaging device (Optos PLC, Dunfermline, United Kingdom) for staging of the DR. High-risk PDR was defined based on the Early Treatment Diabetic Retinopathy Study (ETDRS) as presence of at least 1 of the following: new vessels on the disc (NVD) greater than a one-third of the disc area; and any NVD with vitreous hemorrhage or new vessels elsewhere greater than one-half a disc area with vitreous hemorrhage[17] (Figure 1). If both eyes of a patient were eligible, we included the eye with more severe retinopathy and higher quality images. Exclusion criteria included retinal or choroidal diseases that could confound results, such as glaucoma, high myopia, or eyes with astigmatism >3 diopters; high refractive errors (>6 diopters); or cataracts graded above nuclear opalescence grade 3 or nuclear color grade 3 to avoid optical artifacts that could compromise OCTA image quality. Electronic medical records were reviewed to extract demographic and clinical information.

• **PANRETINAL PHOTOCOAGULATION:** PRP was performed according to the recommendations of the ETDRS group.[18] Green argon laser PRP was delivered through a transequator contact lens (Volk Optical Inc, Mentor, Ohio) using a slit-lamp adapted photocoagulator (Novus Varia, Lumenis, Salt Lake City, Utah), or through a 20-D Volk indirect lens (Volk Optical Inc) using a Keeler indirect ophthalmoscope mounted-photocoagulator (Keeler Instruments Inc., Broomall, Pennsylvania). PRP was performed in 2-3 sessions with an interval of 3 weeks between sessions. The individual spots were spaced 1 laser spot-size apart. Peripherally, the treatment was carried out as far as possible with indirect laser delivery and posteriorly to just outside the arcades. Shots were delivered with a 200-μm spot size and a pulse duration of 0.1 s, for a total of 900-2000 spots. The power of the laser was individually adjusted to produce yellowish white coagulative spots. Treatment was deemed adequate when no further neovascularization or hemorrhage was detected during follow-up visits at 1 month, and at 3 to 6 months after the final laser treatment session.

• **OCTA IMAGING AND SEGMENTATION:** Patients underwent imaging using the RTVue-XR Avanti device (Optovue Inc, Fremont, California), with split-spectrum, amplitude-decorrelation angiography (SSADA) software. This instrument has an A-scan rate of 70,000 scans per second and uses a light source centered at 840 nm and a bandwidth of 45 nm. Two consecutive B-scans (M-B frames), each containing 304 A-scans, were captured at each sampling location. SSADA was used to extract OCTA information. For each patient, we obtained 3- × 3-mm scans centered on the fovea. En face OCT angiograms were segmented automatically using the built-in software (version 2017.1.0.151,

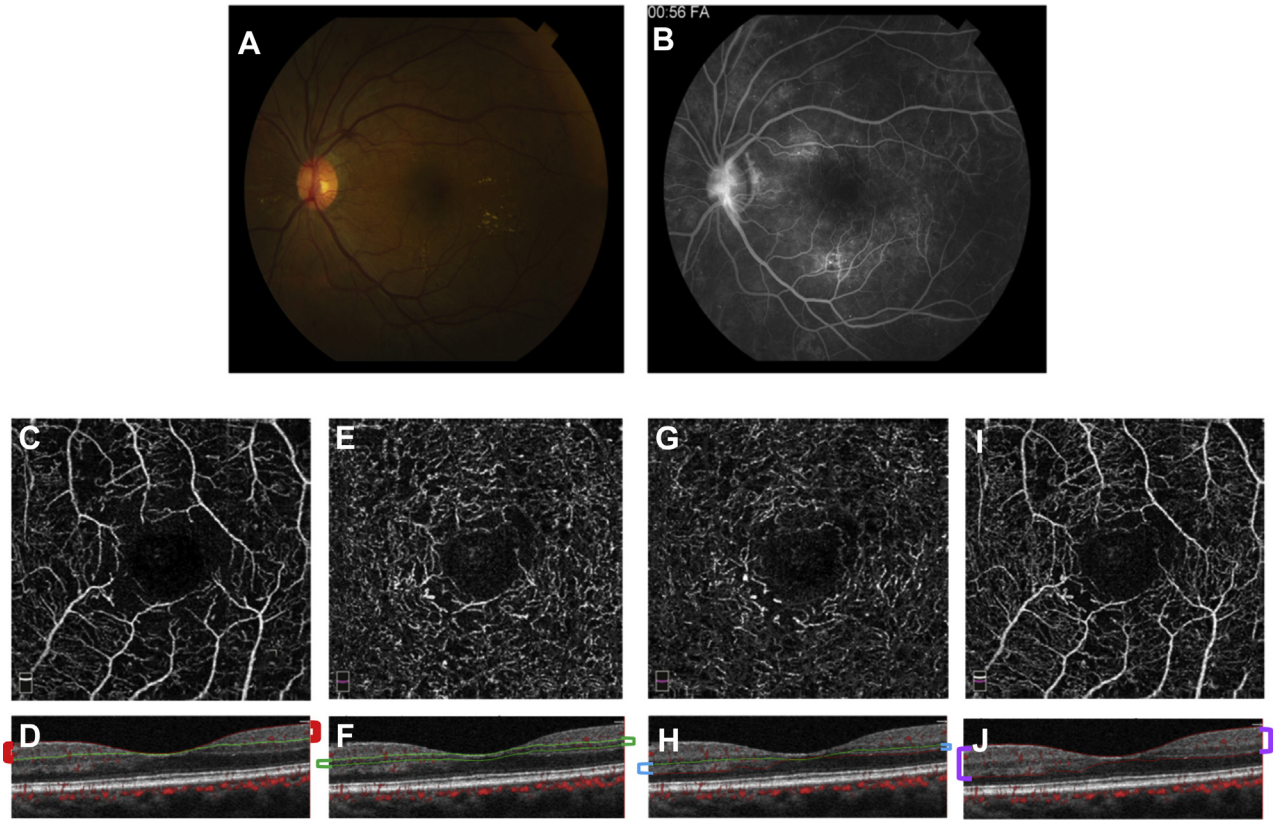


**FIGURE 1. Optical coherence tomography angiography (OCTA) segmentation. A. Fundus photograph of case 7 showing new vessels on the optic disc (NVD) with scattered microaneurysms across the posterior pole, and hard exudates temporal to the fovea. B. Fluorescein angiogram of the same eye during the late phase showing hyperfluorescent leakage of the NVD, as well as hyperfluorescent leaking microaneurysms surrounding the fovea. The foveal avascular zone is enlarged, and there are areas of temporal and inferior peripheral nonperfusion. C-J. *En face* 3- × 3-mm OCTA sections centered on the foveal avascular zone of the same patient with their corresponding B scans, (C and D) segmented to show the superficial (SCP), (E and F) middle (MCP), and (G and H) deep capillary (DVP) plexuses, as well as the (I and J) full retinal thickness. The colored brackets on the sides of the cross-sections outline the relevant segmentation lines in each plexus. For the SCP, the inner boundary was set at the internal limiting membrane (ILM), and the outer boundary at 9 μm above the inner plexiform layer (IPL). The MCP inner boundary was set at 9 μm above the IPL, and the outer boundary at 31 μm below it. The DCP inner boundary started at 31 μm below the IPL, with the outer boundary at 10 μm below the outer plexiform layer (OPL). To obtain the full retinal thickness angiogram, the built-in software uses an inner boundary set at the ILM, and the outer boundary is set at 10 μm below the OPL.**

built-in software 3D- projection artifact removal for artifact removal) to define the SCP and full retinal thickness angiogram. We then performed manual segmentation to segment the deep capillary complex into its individual plexuses, the MCP and DCP. For the SCP, the inner boundary was set at the internal limiting membrane, and the outer boundary was set at 9 μm above the inner plexiform layer (IPL). The MCP inner boundary was set at 9 μm above the IPL, and the outer boundary was set at 31 μm below it. The DCP inner boundary started at 31 μm below the IPL, with the outer boundary at 10 μm below the outer plexiform layer. To obtain the full retinal thickness angiogram, the built-in software uses an inner boundary set at the internal limiting membrane, with the outer boundary at 10 μm below the outer plexiform layer (Figure 1).

Each patient underwent OCTA imaging at 3 time points: at baseline on the same day they received the fluorescein angiography (before initiating PRP), then at 1 month, and at 3-6 months after the last PRP session. Only eyes that had OCTA images without significant movement or shadow artifacts, with a quality index of ≥6 and signal strength index score >50, were considered eligible.

• **VESSEL DENSITY AND CENTRAL FOVEAL THICKNESS:** We used the built-in AngioVue Analytics software (version 2017.1.0.151, OptoVue Inc, Fremont, California, USA) to obtain parafoveal blood VD for the SCP, MCP, DCP, and full retinal thickness angiograms. The parafovea is defined as an annulus centered on the fovea with inner and outer ring diameters of 1 and 3 mm, respectively. VD is reported as the percentage of the total area occupied by blood vessels within the parafovea. To calculate VD, the software extracts a binary image of the blood vessels from the grayscale OCTA image, and then calculates the

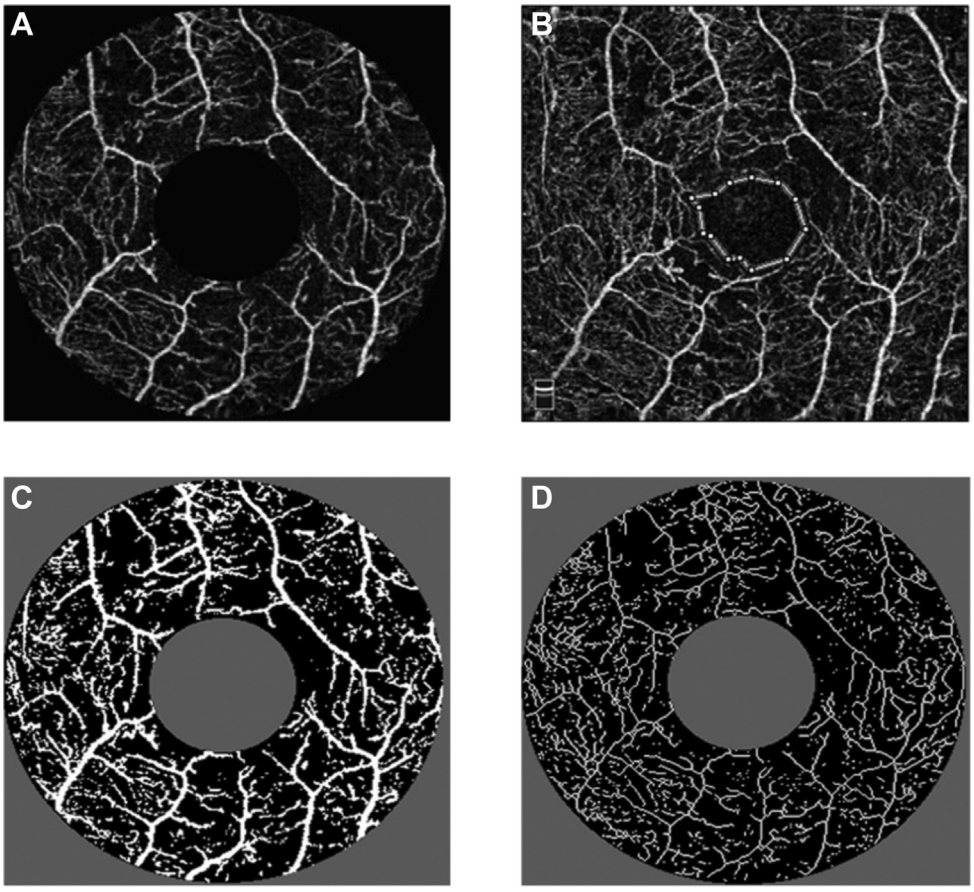


**FIGURE 2. Optical coherence tomography angiography (OCTA) parameters. A. OCTA en face slab of the superficial capillary plexus (SCP) of case 5, processed to demonstrate the parafoveal area between the 1- and 3-mm circles, centered on the foveal avascular zone (FAZ). B. Tracing of the FAZ in the full-thickness retinal slab of the same patient to obtain the average pixel value, representing the noise threshold of the scan. C. Binarization of the SCP slab in (A), using the threshold obtained from (B). This is used to calculate the adjusted flow index and the percentage area of nonperfusion D. Skeletonized vessels of the SCP, where all vessels are 1-pixel wide. This is used to calculate the vessel length density of the SCP.**

percentage of pixels occupied by blood vessels in the defined region. Using the built-in software, the central foveal thickness (CFT)was also recorded.

• **VESSEL LENGTH DENSITY:** For the SCP, we also calculated the vessel length density (VLD), by converting all vessels into a single pixel-wide structure, thereby removing the effect of larger vessels on the overall VD. To calculate the VLD, we exported the SCP angiograms into ImageJ (National Institutes of Health, Bethesda, Maryland).[19] We binarized the angiogram into a black-white image and then we generated a skeletonized image (Figure 2). VLD is measured in units of $mm^{-1}$, using the following equation[20]:

$$\text{VLD} = \text{skeletonized vessel length (mm)}/\text{total area } (\text{mm}^2)$$

• **ADJUSTED FLOW INDEX:** The adjusted flow index (AFI) is an indirect and relative measure of flow velocity based on pixel intensity, which has been shown to correlate to flow velocity in OCTA within a limited range.[21] Two independent graders (A.E.F. and J.G.) extracted these measurements, as previously described.[14,22] Briefly, we exported the SCP, MCP, DCP, and full retinal thickness angiograms into ImageJ (National Institutes of Health).[19] First, we established a global threshold for each eye to distinguish vessels from background noise. On the full retinal thickness angiogram, we selected an area within the foveal avascular zone using a circle with a 30-pixel radius. We obtained the mean pixel intensity within the circle and repeated the process 3 times. We took the average of the 3 selections as the noise level for that eye. All pixels with intensities above the noise level were considered "vessels" and pixels with intensities below the noise level were considered "nonperfusion." The parafovea was marked by creating 1- and 3-mm circles, centered on the anatomical center of the foveal avascular zone. The foveal area (central 1 mm) and the perifoveal area outside the 3-mm circle were excluded, and only the parafoveal area between the 2 circles was used for analysis

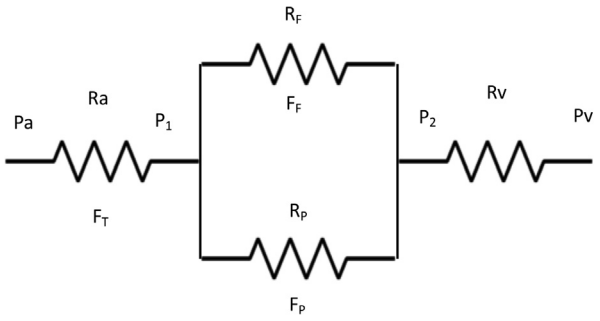


**FIGURE 3. Electrical circuit model of retinal blood flow, vascular resistance, and vascular pressures. To represent the hemodynamics of the retinal vascular network in a mathematical way, we modeled it as an electrical circuit, where the pressure in the central retinal artery and vein (Pa and Pv) represent the pressure input and output of the circuit, respectively. Their respective resistances are represented by Ra and Rv. The total blood flow through the retina (macula and periphery) is represented by $F_T$. Two additional pressure parameters ($P_1$ and $P_2$) represent the pressure in the circuit once the central retinal vessels enter the eye. The macular (para-foveal) and peripheral resistance and flow are represented by $R_F$, $F_F$, $R_P$ and $F_P$, respectively, whereby the macular and peripheral circulations form a parallel circuit.**

(Figure 2). For each of the 4 segmented angiograms, we calculated the parafoveal AFI, which is defined as the average decorrelation value of all pixels above the noise threshold (only vessels) in the en face angiogram of the parafoveal area (Figure 2).[22,23]

• **PERCENT AREA OF NONPERFUSION:** After marking the parafoveal area as described earlier, we exported the SCP, MCP, DCP, and full retinal thickness angiograms into a custom-made MATLAB (MathWorks, Inc., Natick, Massachusetts) code. This software automatically calculated the percentage of pixels in each angiogram below the noise level, or the percent area of nonperfusion (PAN), as previously described.[24] In this study, we used PAN as a metric of the level of nonperfusion in each capillary plexus, adjusted for noise (Figure 2).

• **GRADING AND IMAGE ANALYSIS:** To ensure the validity and repeatability of the results, the images were analyzed by 2 independent graders, who were blinded to eye status (A.E.F. and J.G.). After image acquisition, the images were randomized, and the graders were blinded to the randomization process and to each other's results. An interclass correlation coefficient was calculated for the manually graded parameters, including VLD, AFI, and PAN.

• **STATISTICAL ANALYSIS:** Univariate repeated measures analysis of variance was used to examine the changes in all the recorded parameters comparing the 3 visits. These parameters included 3 parameters in the SCP, MCP, DCP, and full thickness angiograms: VD, AFI, and PAN, as well as VLD of the SCP. To correct for the violation of sphericity, a Greenhouse-Geisser correction was implemented. Post hoc Tukey least significant difference analyses were run for pairwise comparisons. For multivariate analysis, we performed mixed-effect linear regression models, with autoregressive covariance to account for the correlation over time within each patient. In the model, we also adjusted for age and signal strength. A $P$ value of $<.05$ was considered statistically significant.

• **ELECTRICAL CIRCUIT MODEL OF THE RETINAL CIRCULATION:** To represent the hemodynamics of the retinal vascular network in a mathematical way, we modeled the retinal circulation as an electrical circuit, in which pressures are equivalent to voltages, blood flow rates are equivalent to currents, and electrical resistance is equivalent to vascular resistance (Figure 3).

The systemic arterial and venous pressures are Pa and Pv. The pressure inside the eye is lower than Pa,[25] because there is some resistance in the central retinal artery (CRA) that we call $R_a$. Similarly, the venous pressure in the eye must be approximately equal to intraocular pressure, which is higher than systemic venous pressure, Pv, so there is some venous resistance (Rv) between the central retinal vein (CRV) inside the eye, and Pv. $\mathbf{P_a}$ and $\mathbf{P_V}$ represent the pressures at the inlet and outlet of the circuit, respectively. The total blood flow through the retina (fovea and periphery) is represented by $\mathbf{F_T}$. Two additional pressure parameters ($\mathbf{P_1}$ and $\mathbf{P_2}$) represent the pressures at the point where the CRA divides into macular and peripheral circulations and the pressure before the CRV, respectively. The macular (parafoveal) and peripheral resistances and flows are represented by $\mathbf{R_f}$, $\mathbf{F_f}$, $\mathbf{R_p}$, and $\mathbf{F_p}$, respectively. This is highly oversimplified, but the periphery can be considered as a unit for the present purpose because this is where PRP occurs. Expansion of the peripheral circulation into subregions would have no advantage for the illustrative value of the model and would not change the conclusions.

The model assumes that the system has a constant inlet pressure ($\mathbf{P_a}$). Flow then depends on the resistances and is not constant. The only assumption that we introduce regarding the PRP-induced change in this system is increased peripheral resistance after PRP, with peripheral resistance after PRP being higher than before PRP ($\mathbf{R_{pA} > R_{pB}}$). This assumption is well supported by the literature, which shows large vessel constriction and overall decreased retinal blood flow following PRP.

1. Total flow is equal to the difference in arterial and venous pressures divided by the total resistance in the system:

$$F_T = (P_a - P_V)/R_T \quad (1)$$

2. Total resistance is equal to the sum of the resistance of the CRA and vein and the microcirculation (foveal and peripheral):

$$R_T = R_a + R_V + R_M \quad (2)$$

**3. $R_M$** is a parallel combination of foveal and peripheral resistances, or:

$$R_M = \frac{R_F \times R_P}{R_F + R_P} \quad (3)$$

so

$$R_T = R_a + R_V + \frac{R_F \times R_P}{R_F + R_P} \quad (4)$$

After PRP, $R_M$ increases, no matter what the initial values of $R_F$ and $R_P$ were, because of the larger multiplicative effect of $R_P$ in the numerator, so $R_T$ also increases after PRP.

4. Recognizing that the total flow needs to go through the entire circuit, and through Ra and Rv, we can solve for P1 and P2:

$$F_T = (P_a - P_V)/(R_T) = (P_a - P1)/R_a = (P2 - P_V)/R_V \quad (5)$$

$$(P_a - P_1) = \frac{R_a(P_a - P_V)}{R_T} \Rightarrow P_1 = P_a - \frac{R_a(P_a - P_V)}{R_T} \quad (6)$$

$$(P_2 - P_V) = \frac{R_V(P_a - P_V)}{R_T} \Rightarrow P_2 = \frac{R_V(P_a - P_V)}{R_T} + P_V \quad (7)$$

5. Macular (para-foveal) flow ($F_F$), based on the diagram in Figure 3, is:

$$F_F = \frac{P_1 - P_2}{R_F} \quad (8)$$

Peripheral flow is:

$$F_P = \frac{P_1 - P_2}{R_P} \quad (9)$$

## RESULTS

WE CONSECUTIVELY RECRUITED ALL SUBJECTS WHO FIT THE eligibility criteria and who were offered PRP in the course of their clinical care based on diagnosis of high-risk PDR in our practice during the study period. Of the original 13 subjects recruited, 3 eyes with baseline poor quality images and significant artifacts related to vitreous hemorrhage and poor fixation were excluded and were not studied further. The remaining 10 eyes of 10 subjects with treatment-naïve PDR, including 7 men and 3 women, with an average age of 46 years, continued in the study. An overview of the demographic and clinical data are presented in Table 1. Each subject underwent 3 imaging sessions: baseline (before PRP), at 1 month, and at 3-6 months following the last treatment session, for a total of 30 study imaging sessions. Based on quality metrics, 1 session was excluded from the angiographic data analysis, for a total of 29 study sessions for OCTA.

The average measure intraclass correlations obtained for VLD, AFI, and PAN were 0.920, 0.916, and 0.918, respectively.

• **CENTRAL FOVEAL THICKNESS:** Univariate analysis showed a statistically significant difference in CFT between the three visits ($P = .028$) (Table 2), with a significant increase at 1 month compared to baseline, but no difference at 6 months. Using linear regression models adjusted for age and signal strength, only baseline and one month were significantly different, but not the other comparisons.

• **VESSEL DENSITY AND VESSEL LENGTH DENSITY:** There was a trend for decreasing VD at the deeper complex with time following PRP, which on univariate analysis, was not statistically significant (Table 2). With adjusted multivariable models, only the MCP VD was significantly decreased, when comparing baseline with the final follow up.

• **PERCENTAGE AREA OF NONPERFUSION:** PAN, a marker of nonperfusion, showed progressive increase at all layers during follow-up (Table 2). These trends became statistically significant in the adjusted multivariable models, especially when comparing baseline with the final follow-up (Table 3, Figure 4).

• **ADJUSTED FLOW INDEX:** As a surrogate marker for flow, the AFI showed a statistically significant increase in all 4 angiograms (SCP, MCP, DCP, and full thickness) on univariate analysis (Table 2). These findings remained significant in the adjusted multivariable model (Table 3, Figure 4).

• **MATHEMATICAL MODEL RESULTS:** From equations (6) and (7), we can see that because $R_T$ increases, $P_1$ increases and $P_2$ decreases after PRP, whereas everything else in those equations is constant. $\mathbf{P_1\text{-}P_2}$ therefore increases, and this is what drives the increase in macular flow (equation 8) The greater pressure drop across the circulation would also tend to make peripheral flow larger, but it is more than offset by the increase in peripheral resistance ($R_P$), so peripheral flow decreases. These conclusions hold even if either Ra or Rv is small enough that it does not add appreciably to $R_T$, but one of them has to be significant, and this is strongly supported by the measured retinal pressure profiles.[25]

**TABLE 1.** Demographics, Diabetes Status, Ocular, and Clinical Characteristics of Subjects

| Case | Sex | Age | Duration of DM (yrs) | Type of DM | HbA1c (%) | Hypertension | Eye | Lens Status | No. of Laser Spots |
|---|---|---|---|---|---|---|---|---|---|
| 1 | F | 34 | 26 | 1 | 9 | No | OD | Phakic | 1836 |
| 2 | M | 50 | 19 | 2 | 10 | No | OS | Phakic | 1302 |
| 3 | M | 35 | 18 | 1 | 11 | Yes | OS | Phakic | 939 |
| 4 | M | 62 | 34 | 2 | 6.5 | Yes | OD | Pseudophakic | 1063 |
| 5 | F | 38 | 12 | 2 | 11.3 | No | OD | Phakic | 1500 |
| 6 | M | 40 | 14 | 2 | 9.6 | No | OD | Phakic | 932 |
| 7 | M | 52 | 10 | 2 | 8 | No | OS | Pseudophakic | 1231 |
| 8 | M | 44 | 11 | 2 | 6.9 | Yes | OS | Phakic | 1057 |
| 9 | M | 41 | 20 | 2 | 12.3 | No | OD | Phakic | 1837 |
| 10 | F | 66 | 18 | 2 | 11 | No | OD | Pseudophakic | 985 |
| Avg (SD) | | 46 (11) | | | | | | | |

DM = diabetes mellitus; HBA1c = glycosylated hemoglobin.

**TABLE 2.** Univariate Analysis of Optical Coherence Tomographic Angiography Parameters Comparing With Follow-up Visits

| | | | | | Pairwise Comparison | | |
|---|---|---|---|---|---|---|---|
| Parameter | Baseline | 1 Month | 3-6 months | Repeated measures ANOVA (*P* value) | Baseline vs. 1 month | 1 month vs. Final visit | Baseline vs. Final visit |
| CFT | 258.5 ± 35.7 | 277.3 ± 35.6 | 270.6 ± 31.5 | **.03** | **0.03** | **0.02** | 0.07 |
| VD | | | | | | | |
| SCP | 37.11 ± 4.41 | 38 ± 4.90 | 37.6 ± 3.24 | .60 | | - | |
| MCP | 43.98 ± 5.16 | 41.79 ± 7.19 | 39.08 ± 7.08 | .06 | | - | |
| DCP | 49.94 ± 7.55 | 45.06 ± 10.72 | 45.35 ± 9.79 | .28 | | - | |
| Full | 48.04 ± 3.53 | 47.99 ± 4.39 | 48.95 ± 2.84 | .5 | | - | |
| VLD | | | | | | | |
| SCP | 18.56 ± 1.93 | 18.09 ± 1.89 | 18.02 ± 3.05 | .65 | | - | |
| AFI | | | | | | | |
| SCP | 0.47 ± 0.01 | 0.48 ± 0.02 | 0.482 ± 0.02 | **.03** | 0.102 | 0.12 | **0.02** |
| MCP | 0.45 ± 0.02 | 0.47 ± 0.03 | 0.472 ± 0.03 | **.02** | 0.07 | 0.14 | **0.01** |
| DCP | 0.44 ± 0.03 | 0.46 ± 0.03 | 0.468 ± 0.03 | **.004** | **0.03** | 0.11 | **0.006** |
| Full | 0.46 ± 0.02 | 0.47 ± 0.02 | 0.477 ± 0.02 | **.03** | 0.096 | 0.17 | **0.02** |
| PAN | | | | | | | |
| SCP | 33.18 ± 8.84 | 37.75 ± 7.11 | 39.25 ± 7.49 | .15 | | - | |
| MCP | 24.46 ± 6.18 | 29.36 ± 8.49 | 30.86 ± 7.7 | .06 | | - | |
| DCP | 25.16 ± 6.98 | 27.94 ± 8.06 | 30.25 ± 10.72 | .10 | | - | |
| Full | 22.46 ± 6.95 | 25.42 ± 4.38 | 26.93 ± 6.11 | .09 | | - | |
| SSI | 58.3 ± 8.65 | 60.2 ± 8.20 | 59.3 ± 8.77 | .64 | | - | |

AFI = adjusted flow index; ANOVA = analysis of variance; CFT = central foveal thickness; DCP = deep capillary plexus; Full = full retinal thickness; MCP = middle capillary plexus; PAN = percentage area of nonperfusion; SCP = superficial capillary plexus; SSI = signal strength index; VD = vessel density; VLD = vessel length density.

Bold values indicate statistical significance.

## DISCUSSION

IN THIS STUDY, WE USED OCTA TO STUDY THE EVOLUTION of macular capillary changes following PRP therapy and found that the capillary flow (AFI), a measurement of pixel intensity and surrogate marker for blood flow, increased in all capillary levels in the parafovea. This was counterbalanced by an overall trend for decreased capillary density along with a significant increase in capillary nonperfusion.

The effect of PRP on retinal blood flow has been explored in humans, using laser Doppler flowmetry in individual blood vessels.[5] These investigators showed vessel constriction and increased flow velocity in the larger vessels around the optic nerve following treatment. Using a variety of

**TABLE 3.** Multivariable Linear Regression Model of Optical Coherence Tomographic Angiography Parameters Before and After Adjusting for Age and Signal Strength Index

| Parameter | Unadjusted (*P* value) | Adjusted (for age and SSI) | | |
|---|---|---|---|---|
| | | 1 Month vs. Baseline (*P* value) | Final Visit vs. Baseline (*P* value) | Final Visit vs. 1 Month (*P* value) |
| CFT | .004 | **.002** | .09 | .2 |
| VD | | | | |
| SCP | .5 | .57 | .56 | .83 |
| MCP | .1 | .3 | **.03** | .08 |
| DCP | .1 | .1 | .08 | .47 |
| Full | .3 | .4 | .3 | .06 |
| VLD | | | | |
| SCP | .6 | .2 | .3 | .8 |
| AFI | | | | |
| SCP | **.02** | **.01** | **.006** | **.01** |
| MCP | **.02** | **.005** | **.006** | .38 |
| DCP | **.002** | **.0004** | **.0003** | .08 |
| Full | **.02** | **.01** | **.005** | .24 |
| PAN | | | | |
| SCP | .098 | .057 | **.03** | .39 |
| MCP | **.02** | **.01** | **.002** | .19 |
| DCP | **.04** | **.03** | **.002** | **.04** |
| Full | **.04** | **.04** | **.008** | .13 |

AFI = adjusted flow index; CFT = central foveal thickness; DCP = deep capillary plexus; Full = full retinal thickness; MCP = middle capillary plexus; PAN = percentage area of nonperfusion; SCP = superficial capillary plexus; SSI = signal strength index; VD = vessel density; VLD = vessel length density.
Bold values indicate statistical significance.

technologies, other studies showed overall decreased blood flow in eyes with PDR after PRP.[6–10] The efficacy of PRP in PDR is believed to be related to improved inner retinal oxygen delivery with consequent decreased angiogenic drive and regression of neovascularization.[9,26] How these large vessel hemodynamic changes affected blood flow distribution in the macular microvasculature and its sublayers had not been previously accessible to study by the available technology, which did not have the requisite axial resolution that is now available with OCTA.

Our results showed that, in addition to the well-known large vessel hemodynamic changes, there were significant macular capillary modulations in response to PRP. The most significant finding in our study was an increase in a surrogate for capillary flow, quantified as increased pixel intensity, across all capillary layers of the macula, which remained significant after correcting for signal strength and age (Table 3. Figure 4). We believed this was a result of redistribution of blood flow from the periphery to the macular region, along with reorganization of capillary networks following PRP. We did not believe that this was related to a confounding effect of macular edema, because the transiently significant increase in CFT at 1 month became insignificant with further follow-up (Table 2). We acknowledge the caveat that we did not have information on volumetric macular thickness, which would have provided stronger support for this conclusion.

We originally hypothesized that there would be differential changes in the different capillary networks based on our previous work.[14,15] We predicted that the SCP would show decreased blood flow, whereas the deeper capillaries would have an improved flow, as a result of regression of SCP telangiectatic-dilated vessels, and reversal of the potential steal phenomenon.[15] Instead, we found an overall significant increase in flow at all macular capillary plexuses at all timepoints, along with decreased capillary density, especially at the final follow-up. Improved and more effective flow in the remaining capillaries of the macula could be a direct result of closure of the peripheral neovascular and intraretinal microvascular abnormalities, with more effective perfusion of the posterior pole. This finding was not previously accessible to studies that were limited to studying large vessel hemodynamics. This capillary effect could represent a relative normalization and improvement of macular blood flow after the laser procedure.

To further support our experimental results, we sought to mathematically model the effect of PRP on retinal hemodynamics. To do this, we used a simplified electrical circuit simulation, where we represented the macular and peripheral microcirculations by parallel circuits that share common inflow and outflow channels, the pressure in the central arteriolar and venous vasculature, respectively (Figure 3). By assuming that the only change induced by PRP in this model was increased vascular resistance and decreased flow in the peripheral microvasculature, this model showed that PRP would be associated with increased macular flow, thus confirming the present study findings.

In the adjusted multivariable logistic model, we found that the VD was only significantly decreased at a single timepoint in the MCP (Table 3). We originally hypothesized that only the SCP VD would decrease as a result of constriction of the large vessels and regression of the dilated telangiectatic abnormalities, whereas the VLD, which removed the effect of larger vessels, would be unaffected. Interestingly, when we evaluated a nonperfusion metric where we accounted for the level of noise (PAN), there was significant increase in nonperfusion at all capillary levels in the adjusted model (Figure 4). Although we do not have a definitive explanation for this apparent discrepancy, one possibility could be that removal of noise may also artifactually remove the smallest and least perfused capillaries and perhaps lead to falsely elevated nonperfusion. Other possibilities include an underestimation of small capillary changes by the VD metric. This discrepancy is intriguing and remains to be further validated in larger cohorts.

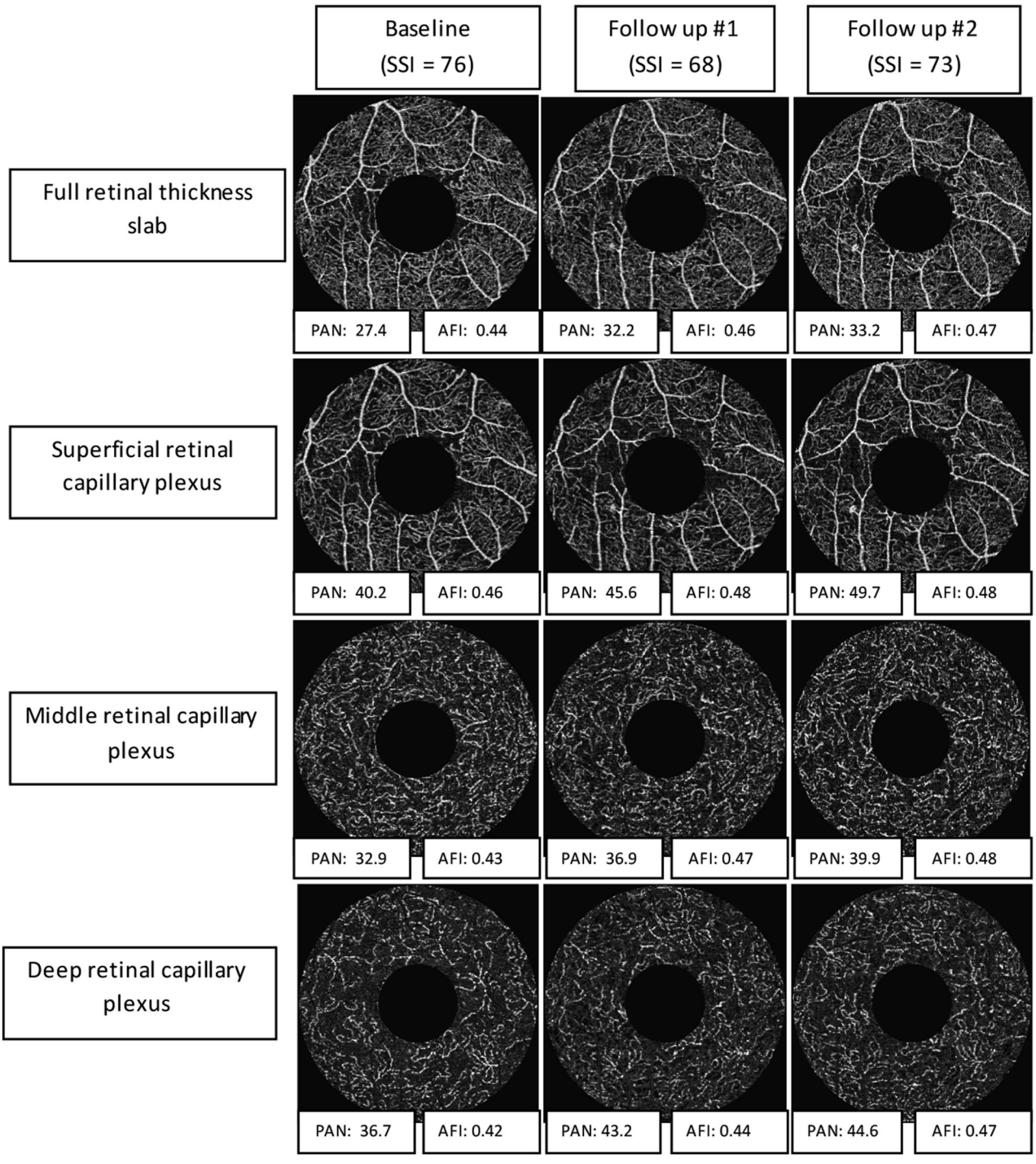


**FIGURE 4. Optical coherence tomography angiography (OCTA) nonperfusion and adjusted flow index (AFI) progression following panretinal photocoagulation (PRP). Example of the change in nonperfusion and flow parameters over time following PRP. Each column represents a timepoint, whereas each row represents a specific plexus. At each timepoint, we highlight the signal strength (SSI), to illustrate the relatively consistent angiogram quality in this eye. In addition, below each angiogram we include the numeric values of the most significant quantitative parameters, percentage area of nonperfusion (PAN) and AFI. This example illustrates the overall results, and shows that after PRP, the relative capillary non-perfusion and flow parameters increase across all capillary plexuses.**

We made every effort to correct for potential confounders in the multivariable model, including age and signal strength. Signal strength has specifically been shown to significantly affect quantitative measurements of retinal capillary density.[27] Other potential confounders that we could not correct for included blood pressure and blood

glucose. It has been shown that high glucose and insulin administration can lead to increased vessel diameters and flow speeds in the retinal vasculature, as well as increased renal blood flow.[28]

Strengths of our study include the strict follow-up and image quality criteria, as well as the detailed analysis. In addition, we analyzed the details of retinal capillary metrics at 3 macular plexuses, which provided robust and consistent results, as well as new information regarding the microvascular consequences of laser PRP in PDR. Furthermore, the mathematical model presented here confirmed that because of the knowledge of increased peripheral resistance and decreased peripheral flow, PRP would be associated with increased blood flow to the macula, and no change in parafoveal vascular resistance was required. Although an increase is predictable, the magnitude of the increase could not be predicted without numerical values of the resistances in the model.

One potential limitation of our study was the use of 3- × 3-mm scans, which do not include the arcades or the entire posterior pole. We focused on these scans because of the current status of the technology and speed constraints that limit these wider scans to sparse scan density that does not provide adequate pixel resolution to resolve the deeper plexuses. Because our hypothesis posited that the changes at the different capillary levels would be distinct, we wanted to maximize the resolution for these deeper plexuses at the expense of wider views.

Future studies to analyze larger data sets are needed to validate our results. In addition, it would be interesting to compare the hemodynamic effects of laser PRP with those of anti- vascular endothelial growth factor therapy, which is the currently proposed alternative to laser therapy in PDR, based on the Diabetic Retinopathy Clinical Research (DRCR)-net studies.[29] Other important future research includes correlating baseline peripheral nonperfusion area with subsequent OCTA changes, assessment of the effect of PRP on fellow eyes, and the implementation of higher speed devices with higher density and wider scans to cover the arcades or beyond. In addition, it would be important to further assess other metrics of macular hemodynamic function, including oxygen saturation. Although blood flow and capillary density provide important information about perfusion, retinal oximetry would provide an important complementary physiologic parameter that would allow us to achieve a comprehensive understanding of the metabolic activity of the inner retina.[16]

In summary, we found that macular capillaries underwent significant changes following PRP with increased blood flow at all capillary levels, as well as an apparent increase in nonperfusion, which suggested an overall more effective perfusion of the posterior pole. These results were validated by our mathematical modeling of the effect of PRP on the retinal hemodynamics. Because of the previously known decreased overall retinal blood flow in PDR and especially following PRP, these results would suggest preferential diversion of this low blood flow to the macular area, leading to an improved macular perfusion following PRP. Our results contribute a new mechanistic and hemodynamic dimension to our understanding of the complex biologic effects of PRP.


## ACKNOWLEDGMENTS

THIS WORK WAS FUNDED IN PART BY NATIONAL INSTITUTES OF HEALTH/NATIONAL INSTITUTE OF DIABETES AND DIGESTIVE and Kidney Disease Study 1DP3DK108248 (A.A.F.) and research instrument support by Optovue, Inc, Fremont, California, USA. The funders had no role in study design, data collection and analysis, data interpretation, decision to publish, or preparation of the manuscript. The authors have completed and submitted the ICMJE form for disclosure of potential conflicts of interest, and none were reported. Contributions of authors: Study design (A.A.F., A.E.F., R.A.L.), data analysis (A.A.F., A.E.F., J.G., F.Y.), drafting of manuscript and critical revisions (A.A.F., A.E.F., R.A.L.).


## REFERENCES


1. Budzynski E, Smith JH, Bryar P, et al. Effects of photocoagulation on intraretinal PO2 in cat. *Invest Ophthalmol Vis Sci* 2008;49(1):380–389.
2. Molnar I, Poitry S, Tsacopoulos M, et al. Effect of laser photocoagulation on oxygenation of the retina in miniature pigs. *Invest Ophthalmol Vis Sci* 1985;26(10):1410–1414.
3. Yu DY, Cringle SJ, Su E, et al. Laser-induced changes in intraretinal oxygen distribution in pigmented rabbits. *Invest Ophthalmol Vis Sci* 2005;46(3):988–999.
4. Lau JC, Linsenmeier RA. Oxygen consumption and distribution in the Long-Evans rat retina. *Exp Eye Res* 2012;102:50–58.
5. Feke GT, Green GJ, Goger DG, et al. Laser Doppler measurements of the effect of panretinal photocoagulation on retinal blood flow. *Ophthalmology* 1982;89(7):757–762.
6. Grunwald JE, Riva CE, Brucker AJ, et al. Effect of panretinal photocoagulation on retinal blood flow in proliferative diabetic retinopathy. *Ophthalmology* 1986;93(5):590–595.
7. Grunwald JE, Brucker AJ, Petrig BL, et al. Retinal blood flow regulation and the clinical response to panretinal photocoagulation in proliferative diabetic retinopathy. *Ophthalmology* 1989;96(10):1518–1522.
8. Yamada Y, Suzuma K, Onizuka N, et al. Evaluation of retinal blood flow before and after panretinal photocoagulation using pattern scan laser for diabetic retinopathy. *Curr Eye Res* 2017;42(12):1707–1712.
9. Lee JC, Wong BJ, Tan O, et al. Pilot study of Doppler optical coherence tomography of retinal blood flow following laser photocoagulation in poorly controlled diabetic patients. *Invest Ophthalmol Vis Sci* 2013;54(9):6104–6111.

10. Mendivil A, Cuartero V. Ocular blood flow velocities in patients with proliferative diabetic retinopathy after scatter photocoagulation. Two years of follow-up. *Retina* 1996; 16(3):222–227.
11. Srinivas S, Tan O, Nittala MG, et al. Assessment of retinal blood flow in diabetic retinopathy using doppler fourier-domain optical coherence tomography. *Retina* 2017;37(11): 2001–2007.
12. Mendivil A, Cuartero V, Mendivil MP. Ocular blood flow velocities in patients with proliferative diabetic retinopathy and healthy volunteers: a prospective study. *Br J Ophthalmol* 1995; 79(5):413–416.
13. Cuypers MH, Kasanardjo JS, Polak BC. Retinal blood flow changes in diabetic retinopathy measured with the Heidelberg scanning laser Doppler flowmeter. *Graefes Arch Clin Exp Ophthalmol* 2000;238(12):935–941.
14. Nesper PL, Roberts PK, Onishi AC, et al. Quantifying microvascular abnormalities with increasing severity of diabetic retinopathy using optical coherence tomography angiography. *Invest Ophthalmol Vis Sci* 2017;58(6):BIO307–BIO315.
15. Onishi AC, Nesper PL, Roberts PK, et al. Importance of considering the middle capillary plexus on OCT angiography in diabetic retinopathy. *Invest Ophthalmol Vis Sci* 2018;59(5): 2167–2176.
16. Nesper PL, Soetikno BT, Zhang HF, et al. OCT angiography and visible-light OCT in diabetic retinopathy. *Vision Res* 2017;139:191–203.
17. Grading diabetic retinopathy from stereoscopic color fundus photographs–an extension of the modified Airlie House classification. ETDRS report number 10. Early Treatment Diabetic Retinopathy Study Research Group. *Ophthalmology* 1991;98(5 Suppl):786–806.
18. Early photocoagulation for diabetic retinopathy: ETDRS report number 9. Early Treatment Diabetic Retinopathy Study Research Group. *Ophthalmology* 1991;98(5):766–785.
19. Rasband WS. *Imagej*, US National Institutes of Health, Bethesda, Maryland, USA. Available at: https://imagej.nih.gov/ij/. Accessed July 13, 2018.
20. Samara WA, Shahlaee A, Adam MK, et al. Quantification of diabetic macular ischemia using optical coherence tomography angiography and its relationship with visual acuity. *Ophthalmology* 2017;124(2):235–244.
21. Tokayer J, Jia Y, Dhalla A-H, et al. Blood flow velocity quantification using split-spectrum amplitude-decorrelation angiography with optical coherence tomography. *Biomed Opt Express* 2013;4(10):1909–1924.
22. Alten F, Heiduschka P, Clemens CR, et al. Exploring choriocapillaris under reticular pseudodrusen using OCT-Angiography. *Graefes Arch Clin Exp Ophthalmol* 2016;254(11): 2165–2173.
23. Jia Y, Tan O, Tokayer J, et al. Split-spectrum amplitude-decorrelation angiography with optical coherence tomography. *Opt Express* 2012;20(4):4710–4725.
24. Nesper PL, Soetikno BT, Fawzi AA. Choriocapillaris nonperfusion is associated with poor visual acuity in eyes with reticular pseudodrusen. *Am J Ophthalmol* 2017; 174:42–55.
25. Glucksberg MR, Dunn R. Direct measurement of retinal microvascular pressures in the live, anesthetized cat. *Microvasc Res* 1993;45(2):158–165.
26. Stefansson E. The therapeutic effects of retinal laser treatment and vitrectomy. A theory based on oxygen and vascular physiology. *Acta Ophthalmol Scand* 2001;79(5): 435–440.
27. Lim HB, Kim YW, Kim JM, et al. The importance of signal strength in quantitative assessment of retinal vessel density using optical coherence tomography angiography. *Sci Rep* 2018;8(1):12897.
28. Luksch A, Polak K, Matulla B, et al. Glucose and insulin exert additive ocular and renal vasodilator effects on healthy humans. *Diabetologia* 2001;44(1):95–103.
29. Writing Committee for the Diabetic Retinopathy Clinical Research Network, Gross JG, Glassman AR, et al. Panretinal photocoagulation vs intravitreous ranibizumab for proliferative diabetic retinopathy: a randomized clinical trial. *JAMA* 2015;314(20):2137–2146.